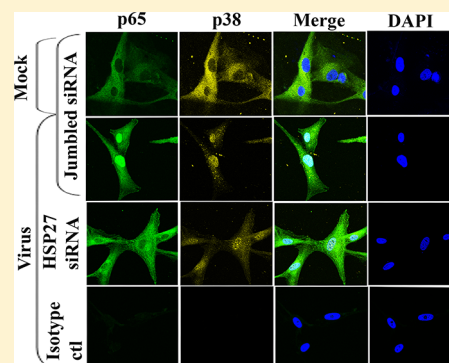


## Heat Shock Protein 27 Mediated Signaling in Viral Infection

Jaya Rajaiya, Mohammad A. Yousuf, Gurdeep Singh, Heather Stanish, and James Chodosh\*

Howe Laboratory, Mass Eye and Ear Infirmary, Department of Ophthalmology, Harvard Medical School, Boston, Massachusetts 02114, United States

**ABSTRACT:** Heat shock proteins (HSPs) play a critical role in many intracellular processes, including apoptosis and delivery of other proteins to intracellular compartments. Small HSPs have been shown previously to participate in many cellular functions, including IL-8 induction. Human adenovirus infection activates intracellular signaling, involving particularly the c-Src and mitogen-activated protein kinases [Natarajan, K., et al. (2003) *J. Immunol.* 170, 6234–6243]. HSP27 and MK2 are also phosphorylated, and c-Src, and its downstream targets, p38, ERK1/2, and c-Jun-terminal kinase (JNK), differentially mediate IL-8 and MCP-1 expression. Specifically, activation and translocation of transcription factor NF $\kappa$ B-p65 occurs in a p38-dependent fashion [Rajaiya, J., et al. (2009) *Mol. Vision* 15, 2879–2889]. Herein, we report a novel role for HSP27 in an association of p38 with NF $\kappa$ B-p65. Immunoprecipitation assays of virus-infected but not mock-infected cells revealed a signaling complex including p38 and NF $\kappa$ B-p65. Transfection with HSP27 short interfering RNA (siRNA) but not scrambled RNA disrupted this association and reduced the level of IL-8 expression. Transfection with HSP27 siRNA also reduced the level of nuclear localization of NF $\kappa$ B-p65 and p38. By use of tagged p38 mutants, we found that amino acids 279–347 of p38 are necessary for the association of p38 with NF $\kappa$ B-p65. These studies strongly suggest that HSP27, p38, and NF $\kappa$ B-p65 form a signalosome in virus-infected cells and influence downstream expression of pro-inflammatory mediators.



Heat shock proteins (HSPs) target other proteins to the proteasome for degradation,<sup>1</sup> bind and refold denatured proteins to prevent apoptosis, and chaperone proteins to distinct cellular compartments.<sup>2,3</sup> HSP27 is a widely expressed protein and one of 10 members of a small HSP family that includes the lens protein  $\alpha$ A- $\alpha$ B crystalline and shares a conserved C-terminal domain.<sup>4</sup> HSP27 is activated upon infection,<sup>5–8</sup> can mediate either cytoskeletal stability or cell motility,<sup>9–12</sup> and prevents apoptosis.<sup>2,13–19</sup> HSP27 is required for IL-1-induced expression of the pro-inflammatory mediators IL-6, IL-8, and cyclooxygenase-2.<sup>20,21</sup> HSP27 is also linked to various signaling pathways involved in development,<sup>22,23</sup> differentiation, and cell growth.<sup>24–26</sup>

Nuclear factor  $\kappa$ B (NF- $\kappa$ B) is a well-studied transcription factor within a five-member family, including RELA (NF $\kappa$ B-p65), RELB, c-REL, NF- $\kappa$ B1 (P50/100), and NF- $\kappa$ B2 (p52/105), and is important to the expression of significantly more than 100 genes. The majority of these participate in regulation of innate and adaptive immunity.<sup>27,28</sup> In viral infection, NF $\kappa$ B induces strong transcriptional stimulation of both viral and cellular genes.<sup>5,29–31</sup> Chemokine induction in infection is controlled by NF $\kappa$ B transcription factors through formation of specific homo- or heterodimers for transcriptional activation of target genes in a cell specific manner. We have earlier shown the kinetics of IL-8 and MCP-1 expression upon infection relate directly to the differential regulation of specific NF $\kappa$ B dimers.<sup>32</sup>

Mitogen-activated protein kinases (MAPKs) are activated by serial phosphorylation of upstream kinases upon cellular stimulation by pro-inflammatory cytokines and cellular stresses.

Three major members of the MAPK family, ERK, p38, and JNK, have a conserved domain near the C-terminal region, just outside the catalytic domain, used for docking to their upstream activators, MAPKKs and MEKs,<sup>33,34</sup> their inactivators, MKPs,<sup>35</sup> and their substrates, MAPKAPKs.<sup>33,36</sup> If the aspartic acids at positions 313, 335, and 316 are replaced experimentally with asparagines, binding to other kinases is abrogated.<sup>37</sup> Residues 272–364 at the C-terminus of p38 $\alpha$  are required for TAB1 binding, which leads to autophosphorylation.<sup>38</sup> Phosphorylation of Tyr323 at the C-terminus of p38 $\alpha$  also leads to p38 autoactivation.<sup>36,39</sup>

Adenoviruses have been utilized to study a broad range of cellular functions, including post-transcriptional modification and oncogenesis.<sup>40</sup> Human adenovirus type 37 (HAdV-D37) is an important ocular pathogen,<sup>41–44</sup> and like HAdV-D19 (C), is known to mediate multiple signal transduction events, including activation of Src, MAPKs, and NF $\kappa$ B in corneal cells.<sup>5,32,45</sup> In this study, we show that p38 MAPK, HSP27, and NF $\kappa$ B-p65 play interdependent roles in chemokine induction upon viral infection, in which HSP27 mediates an interaction between the C-terminal region of p38 MAPK and NF $\kappa$ B-p65.

## EXPERIMENTAL PROCEDURES

**Antibodies and Reagents.** Antibodies to p38, HSP27, MAPKAP2, NF $\kappa$ B-p65, I $\kappa$ B, phospho-p38, phospho-HSP27,

Received: May 30, 2012

Revised: June 25, 2012

Published: June 27, 2012

phospho-MAPKAP2, phospho-NF $\kappa$ B-p65, and phospho-I $\kappa$ B were obtained from Cell Signaling Technology (Beverly, MA) and Santa Cruz Biotechnology (Delaware, CA). The anti-human IL-8 antibody and biotin-conjugated anti-human IL-8 antibody were from BD PharMingen (San Diego, CA). NF $\kappa$ B-p65 specific and jumbled control siRNA were purchased from Imgenex (San Diego, CA). The NF $\kappa$ B-NLS mutant was a kind gift from Dr. Fagerlund (National Public Health Institute, Helsinki, Finland). Hsp27 siRNA was constructed as described below.

**Cell Culture and Viruses.** Primary keratocytes were derived from donor corneas as previously described.<sup>46</sup> Briefly, after mechanical debridement of the corneal epithelium and endothelium, corneas were cut into 2 mm diameter sections and placed in individual wells of six-well Falcon tissue culture plates with DMEM (Gibco, Grand Island, NY) supplemented with 10% FBS (Atlanta Biologicals, Lawrenceville, GA), penicillin G sodium, and streptomycin sulfate (Gibco) at 37 °C in 5% CO<sub>2</sub>. Cells from multiple donors were pooled and the cell monolayers used at passage three. The protocol for use of corneas from deceased human donors was approved by the Massachusetts Eye and Ear Human Studies Committee and conformed to the tenets of the Declaration of Helsinki. HAdV-D37 strain GW<sup>44</sup> was obtained from the American Type Culture Collection (ATCC, Manassas, VA) and grown in A549 cells [lung carcinoma cells, CCL 185 (American Type Culture Collection)] in MEM with 2% FBS, penicillin G sodium, and streptomycin sulfate. Virus was purified from A549 cells with a CsCl gradient, dialyzed against a 10 mM Tris (pH 8.0) buffer that contained 80 mM NaCl, 2 mM MgCl<sub>2</sub>, and 10% glycerol, titered in triplicate, and stored at -80 °C.

**Viral Infection.** Monolayer cells grown to 95% confluence in six-well plates were washed in DMEM with 2% FBS and infected with purified HAdV-D37 at a multiplicity of infection (MOI) of 10 or mock-infected with virus-free dialysis buffer as a control. Virus was adsorbed at 37 °C for 1 h and then incubated for an additional 1 h before RNA isolation. For protein analysis, cells grown to 95% confluence in six-well plates were serum-starved for 18–24 h before infection and then lysed postinfection at indicated time points.

**Immunoprecipitation Analysis.** Whole-cell lysates from infected primary keratocytes (300  $\mu$ g) were precleared with protein A-Sepharose beads for 30 min. Precleared protein extracts were added to anti-p38/HA (Santa Cruz Biotechnology) or isotype control (anti-rabbit) antibodies in phosphate-buffered saline containing protease inhibitors [phenylmethylsulfonyl fluoride ( $5 \times 10^{-5}$  M), leupeptin ( $1 \times 10^{-2}$  mg/mL), aprotinin ( $5 \times 10^{-3}$  mg/mL), and sodium vanadate (30 mM)] and 0.1% Tween 20 and rocked at 4 °C for 2 h before the addition of protein A-Sepharose (25  $\mu$ L, 1:1 slurry) and further incubation at 4 °C for 12 h. Immunoprecipitates were washed five times with wash buffer [100 mM Tris-HCl, 500 mM NaCl, and 0.1% Tween 20 (pH 8)] containing protease inhibitors, and proteins were eluted by the addition of sodium dodecyl sulfate–polyacrylamide gel electrophoresis (SDS–PAGE) sample buffer and boiling for 5 min. Samples were run on 10% SDS–PAGE gels using standard protocols and transferred to nitrocellulose membranes (Bio-Rad, Hercules, CA). The membranes were probed with anti-phospho-p65/myc, and the bands were visualized with an enhanced chemiluminescence kit (Amersham, Piscataway, NJ) using Kodak (Rochester, NY) Image Station 4000R.

**Immunoblot Analysis.** HAdV-D37 and mock-infected keratocytes were lysed with chilled cell lysis buffer [20 mM Tris (pH 7.4), 150 mM NaCl, 1 mM EDTA, 1 mM EGTA, 1% Triton X-100, 2.5 mM sodium pyrophosphate, 1 mM  $\beta$ -glycerol phosphate, 1 mM Na<sub>3</sub>VO<sub>4</sub>, 1  $\mu$ g/mL leupeptin, and 1 mM PMSF] and incubated at 4 °C for 5 min. The cell lysates were cleared by centrifugation at 21000g for 15 min. Nuclear and cytoplasmic extracts were prepared using the NucBuster protein extraction kit (Novagen, Darmstadt, Germany). The protein concentration of each supernatant was measured by BCA analysis (Pierce, Rockford, IL) and equalized. Twenty micrograms of cell lysates was subsequently separated by 10% SDS–PAGE and transferred onto nitrocellulose membranes (Bio-Rad). The bands were visualized with an enhanced chemiluminescence kit (Amersham). Densitometric analysis of immunoblots where indicated was performed using ImageQuant 5.2 (Amersham) in the linear range of detection, and absolute values were then normalized to total protein or actin as indicated in figure legends.

**Enzyme-Linked Immunosorbent Assay (ELISA).** The cell supernatants were collected 4 h postinfection, and the levels of IL-8 were quantified by a sandwich ELISA. The detection limit was 30 pg/mL. Plates were read on a SpectraMax M2 microplate reader (Molecular Devices, Sunnyvale, CA) and analyzed with SOFTmax analysis software (Molecular Devices). The means of triplicate ELISA values for each of the virus- and mock-infected wells were compared by ANOVA with Scheffe's multiple-comparison test.

**Confocal Microscopy.** Keratocytes were grown on slide chambers (Nunc, Rochester, NY) and infected with HAdV-D37 or virus-free dialysis buffer for 20 min. Cells were partially fixed in 0.05% paraformaldehyde for 10 min, washed in PBS containing 2% FBS, and permeabilized in 0.1% Triton X-100 for 5 min. After being blocked for 30 min in 3% FBS-PBS, the cells were incubated in 5  $\mu$ g/mL anti-NF $\kappa$ B-p65 or p38 primary antibody for 1 h at room temperature, washed, and incubated in Alexafluor-488- or Alexafluor-594-conjugated secondary antibody, respectively (Molecular Probes, Eugene, OR), for an additional 1 h at room temperature. Cells were then washed, fixed in 2% paraformaldehyde, and mounted using Vectashield mounting medium (Vector laboratories, Burlingame, CA) containing DAPI. Images were taken on an Olympus FluoView 500 (FV500) confocal microscope using a 60 $\times$  water immersion objective. Similarly tagged antibodies against Myc and HA were also used in place of primary antibodies where appropriate in transfection experiments.

**Constructs and Modeling.** Three regions in the HSP27 gene were targeted to construct siRNA using GenScript siRNA target finder (GenScript, Piscataway, NJ). Sequences 5'aagtgggtgacatccagg3' (siRNA293), 5'tgtatttccgcgtgaagca3' (siRNA409), and 5'ggtgactggggtggtgatc3' (siRNA533) were cloned into the pRNAT-U6.2 vector (GenScript) using the BamHI/XhoI site. Clones were then sequenced to validate the construct used in the experiments.

Two C-terminal mutants of p38 were generated:  $\Delta$ R2, with a deletion of amino acids 313–347, that lacks the N-terminally oriented domains of the  $\alpha$ L16 helix and the L16 loop<sup>47</sup> and  $\Delta$ R3, with a deletion of amino acids 279–347, that also removes the C-terminal domains of the  $\alpha$ H and  $\alpha$ I helices.<sup>36</sup> To generate p38 mutants, a forward primer with the Kozak sequence 5'gtgtaccgccgccaccatgtctca3' was used, along with the reverse primers R2 (5'gcgccgcacatcgtggtgactgagcaagta3') and R3 (5'gcgccgcacattggcacaataatac3'). The polymerase chain

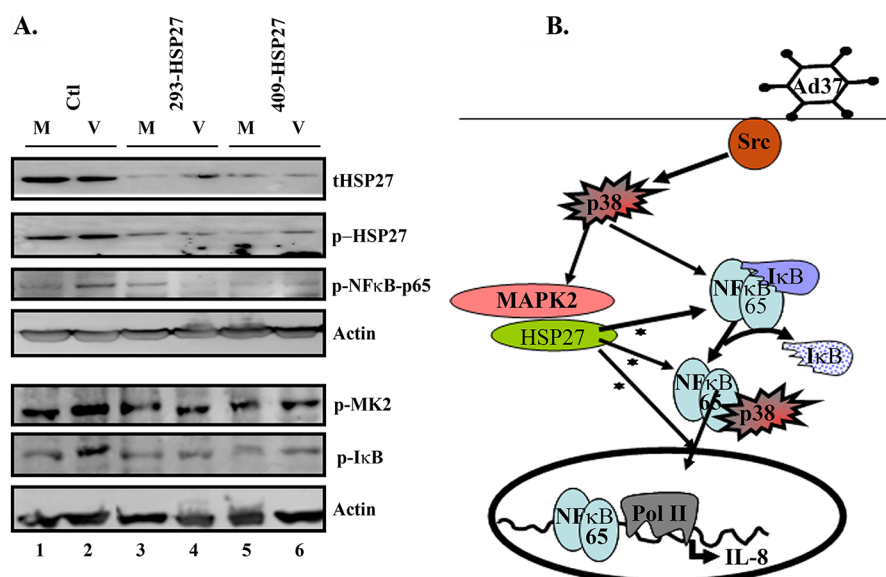


**Figure 1.** Necessity for HSP27 in NFκB-p65 activation. (A) Cells transiently expressing HSP27 siRNA targeted to either of two regions (293 and 409) were infected at a MOI of 10 for 4 h. Cells were then lysed and proteins separated on a 10% SDS–PAGE gel. Virus infection increased the level of phosphorylation of HSP27, NFκB-p65, MK2, and IκB (lane 2). HSP27 specific siRNA (293 and 409), but not scrambled siRNA (Ctl), knocked down the levels of total and phosphorylated HSP27 (tHSP27 and p-HSP27, respectively) in both mock-infected (M) and virus-infected (V) cells. Infection-associated phosphorylation of NFκB-p65 and IκB was also inhibited by HSP27 specific siRNA, but not phosphorylation of MK2. Actin immunoblotting was used to show equivalent protein loaded in each lane. (B) Schematic diagram of the role of HSP27 in signaling in HAdV infection. Previously published data show that p38 is activated by upstream activation of Src upon viral infection. In the data reported here, we show a role for HSP27 (asterisk) in the activation of NFκB-p65 and IκB, association of NFκB-p65 and p38, and nuclear translocation of NFκB-p65 and p38.

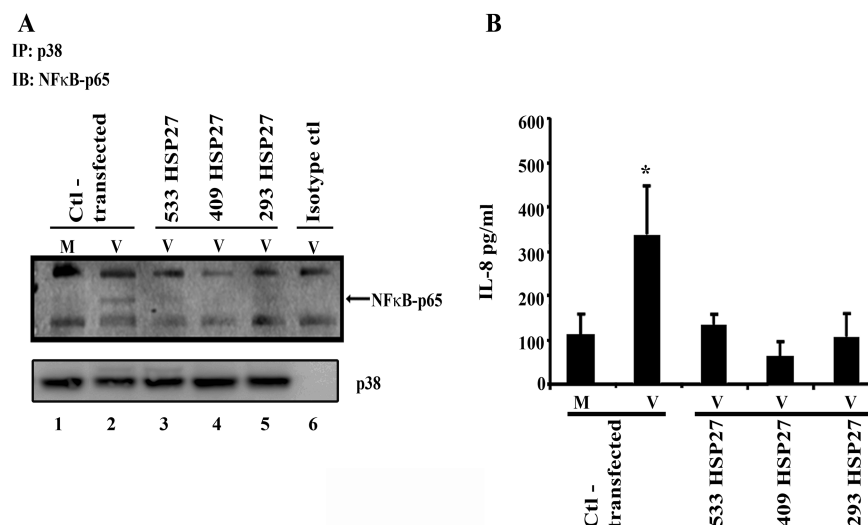


**Figure 2.** Necessity for HSP27 in p38 and NFκB-p65 association, and IL-8 expression, during HAdV infection. (A) Control siRNA (Ctl)- and HSP27 siRNA-transfected cells were infected or mock infected for 4 h and the cell lysates subjected to immunoprecipitation using the anti-p38 antibody followed by immunoblotting with the anti-NFκB-p65 antibody. In virus-infected (V) but not mock-infected (M) cells, NFκB-p65 was successfully coprecipitated with the anti-p38 antibody (lane 2), which is not apparent in mock-infected cells (lane 1) or in HSP27 siRNA-transfected cells (lanes 3–5). A control rabbit IgG did not pull down NFκB-p65. An equal quantity of total p38 protein was evident for all treatment groups. (B) Culture supernatants were collected from the same experiments, and a sandwich ELISA was performed to detect soluble IL-8. Infected cells produced more IL-8 compared to mock-infected cells, and the level of IL-8 expression was reduced to the level of mock-infected cells by HSP27 specific siRNA [ $*p < 0.05$  (ANOVA)].

reaction (PCR) product was generated using the primers mentioned above, digested with NotI and KpnI, and cloned into the pHM6-HA vector (Roche, Indianapolis, IN), containing selection markers neomycin and ampicillin. The construct was verified by DNA sequencing and purified using a plasmid purification kit (Qiagen, Valencia, CA). Protein

structure models of the resultant ΔR2 and ΔR3 mutants of p38 were constructed using SWISS-MODEL (<http://swissmodel.expasy.org/>) for homology modeling.<sup>48</sup> The crystal structure of p38 α MAP kinase<sup>49</sup> [Protein Data Bank (PDB) entry 1WBS] was used as a template for the model, being 100% identical with the mutants except for the indicated deletions.



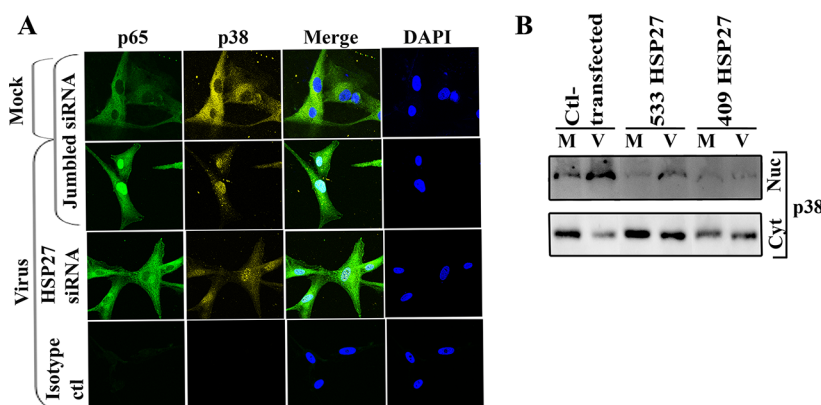


**Figure 3.** Role for HSP27 in nuclear translocation of NFκB-p65 and p38. (A) Cells were transfected with HSP27 specific or scrambled siRNA and 36 h later infected for 30 min. As compared to mock infection (row 1), virus infection induces nuclear translocation of both NFκB-p65 and p38 (row 2). HSP27 siRNA transfection inhibited NFκB-p65 nuclear translocation but only partially inhibited p38 nuclear translocation (row 3). Isotype control (ctl) antibody immunostaining is shown in row 4. (B) Western blot analysis of cytoplasmic (Cyt) and nuclear (Nuc) extracts from mock-infected (M) or virus-infected (V) cells, pretransfected with control or HSP27 specific siRNA, demonstrates partial inhibition of p38 nuclear translocation.

Visualization and analysis were performed with UCSF Chimera (<http://www.cgl.ucsf.edu/chimera>).<sup>50</sup>

**siRNA Transfection.** Transfections were conducted using Oligofectamine (Invitrogen, Carlsbad, CA) following the manufacturer's protocol. Briefly, the transfection mixture was prepared by mixing 12  $\mu$ L of Oligofectamine with 48  $\mu$ L of Opti-MEM (Invitrogen) and incubation at room temperature for 5 min, followed by addition of 100 nM SMARTpool p38-MAPK siRNA or control siRNA (Upstate, Charlottesville, VA), and further incubated for 15 min at room temperature. The transfection complex was then added to cells at 50–70% confluence. Virus infections were conducted 48 h post-transfection. Supernatants and cell lysates were collected 4 h after infection for IL-8 ELISA and p38 Western blot analysis, respectively.

## RESULTS

**HSP27-Dependent Activation of NFκB.** In adenovirus infection, we previously showed by an electron mobility shift assay that NFκB-p65 and cREL bind the IL-8 and MCP-1 promoters, respectively, in a time-dependent fashion and that NFκB-p65 is phosphorylated relative of total p65.<sup>32</sup> In the absence of any external stimuli, NFκB components are sequestered in the cytoplasm by a tight association with inhibitory proteins of the IκB family. Upon stimulation, IκB is phosphorylated by IKK-containing complexes, releasing NFκB subunits and leading to the degradation of IκB via the ubiquitin–proteasome pathway<sup>51</sup> and translocation of NFκB to the nucleus for specific transcriptional activity. This process has been shown to involve HSP27.<sup>1</sup> We transfected HSP27 siRNA into primary keratinocytes and infected them with virus or buffer control 48 h post-transfection. At 1 h post-adenovirus infection, the level of phosphorylation of both NFκB-p65 and IκB was increased (Figure 1). The level of phosphorylation of p65 and IκB was reduced by two distinct HSP27 siRNA constructs where the level of expression of HSP27 was knocked down to 80–90% (Figure 1A and data not shown). As expected, MK2, a kinase upstream to HSP27, was not substantially affected by HSP27 knockdown. A hypothetical model of these interactions, based on the existing literature and confirmed in part by the data in Figure 1A, is shown in Figure 1B.

**HSP27-Mediated Association of NFκB with p38.** In general, NFκB transcription factors are activated rapidly, within minutes, after virus infection.<sup>5</sup> This activation results in a strong transcriptional upregulation of a multitude of early viral and cellular genes.<sup>52</sup> In virus-infected cells, p38 and NFκB-p65 could be co-immunoprecipitated (Figure 2A, lane 2); no such effect was seen in mock-infected (buffer-treated) cells (lane 1). Upon transfection of HSP27 siRNA, this association was prevented (Figure 2A, lanes 3–5). An equivalent amount of p38 was seen in all the immunoprecipitations (Figure 2A), except in the isotype control (lane 6). These data indicate that p38 and NFκB-p65 form a complex only upon viral infection, and that HSP27 is necessary for the association. Culture supernatants were also collected after infection and subjected to an ELISA for IL-8, a paradigm neutrophil chemokine shown in prior studies to be among the first inflammatory mediators upregulated by adenovirus-induced signaling.<sup>5,45</sup> A significant increase in the level of IL-8 expression was observed in virus-infected cells compared to that of buffer-treated cells (Figure 2B). HSP27 siRNA transfection reduced the level of IL-8 expression to that of mock-infected cells [ $p < 0.05$  (ANOVA)].

**HSP27-Dependent Cellular Localization of NFκB-p65.** NFκB and IκB shuttle continually between the cytoplasm and nucleus under steady state conditions, resulting in a basal level of NFκB activity.<sup>53</sup> We previously demonstrated an increased level of nuclear localization of NFκB-p65 upon adenoviral infection.<sup>5</sup> By confocal microscopy, in virus-infected cells pretreated with HSP27 siRNA, NFκB-p65 failed to localize in the nucleus (Figure 3A, row 3). In contrast, virus-infected cells pretreated with control siRNA showed an increased level of nuclear localization of NFκB-p65 (Figure 3A, row 2). Therefore, HSP27 is necessary for the translocation of NFκB-p65 into the nucleus upon viral infection. We also observed fluorescence for p38 in the nucleus upon viral infection (Figure 3A, row 2), but HSP27 siRNA only partially reduced the level of p38 translocation (Figure 3A, row 3). Western blot analysis confirmed the partial inhibition of p38 translocation by HSP27 siRNA (Figure 3B). p38 was previously reported to shuttle to the nucleus from the cytoplasm with an Akt and MK2 complex.<sup>3,54</sup> Our results indicate that NFκB-p65 nuclear localization is dependent upon HSP27 but suggest that p38 may utilize other pathways in addition to HSP27 to translocate to the nucleus.

**HSP27-Independent p38 Translocation of NF $\kappa$ B-p65 in Viral Infection.** We transfected HA-tagged p38 and Myc-tagged NF $\kappa$ B-p65 to further dissect nuclear translocation of p38 and NF $\kappa$ B-p65 upon viral infection. p38 does not have a nuclear localization sequence (NLS), and it is unclear how it translocates to the nucleus upon viral infection. When Myc-tagged NF $\kappa$ B-p65 and HA-tagged p38 were cotransfected, followed by virus infection, both p38 and NF $\kappa$ B-p65 were observed in the nucleus (Figure 4, row 2). Transfection of a

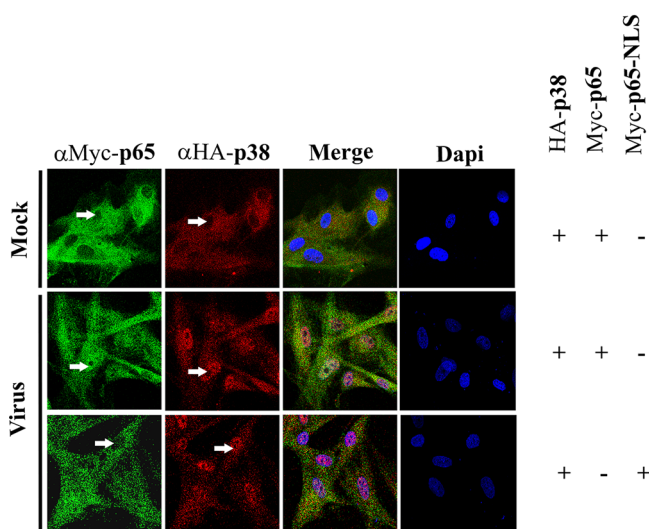


**Figure 4.** Relationship between p38 nuclear translocation and NF $\kappa$ B-p65 activation. HA-p38 and either Myc-NF $\kappa$ B-p65 or Myc- $\Delta$ NLS NF $\kappa$ B-p65 were cotransfected followed 48 h later by virus or mock infection. Cells were then treated with anti-HA and anti-Myc antibodies. Both Myc-NF $\kappa$ B-p65 and HA-p38 localized to the nucleus upon virus infection (arrows, row 2). Myc-tagged p65 failed to translocate to the nucleus when it lacked the nuclear localization signal (Myc- $\Delta$ NLS NF $\kappa$ B-p65) (arrow, column 1, row 3), but in Myc- $\Delta$ NLS NF $\kappa$ B-p65-transfected cells, HA-p38 showed some nuclear localization (column 2, row 3). Columns 3 and 4 show merged images and DAPI staining, respectively.

Myc-tagged NLS mutant of p65 prevented the expression of p65 in the nucleus (Figure 4, row 3) but did not appear to reduce the level of translocation of HA-tagged p38 to the nucleus (Figure 4, row 3). Although not conclusive, these experiments indicate that p38 can enter the nucleus without the aid of NF $\kappa$ B-p65. We cannot exclude the effect of endogenous NF $\kappa$ B-p65 on p38 translocation.

**Importance of the C-Terminus of p38 to the Association of NF $\kappa$ B-p65 with p38.** The p38 molecule is composed of a 135-residue N-terminal domain and a 225-residue C-terminal domain. The N-terminal domain is composed mostly of  $\beta$ -sheets, while the C-terminal domain is largely helical.<sup>36,55</sup> The C-terminus of p38 was shown previously to bind other kinases and is the site of autophosphorylation.<sup>36</sup> We deleted the two helices closest to the C-terminus ( $\Delta$ R2) and, in another mutant, a larger portion encompassing  $\Delta$ R2 and the two adjacent helices ( $\Delta$ R3) to study potential NF $\kappa$ B-p65 binding sites on the p38 molecule. A schematic diagram of the mutants and the amino acid sequences deleted in each mutant are shown in panels A and B of Figure 5, respectively. Western blotting confirmed the expression of both mutants (Figure 5C). Cells were infected 36 h post-cotransfection with Myc-NF $\kappa$ B-p65 and one HA-tagged

p38 mutant or another. Immunoprecipitation analysis showed that the  $\Delta$ R3 p38 mutant with deletion of four helices at the C-terminus, specifically amino acids 279–347, reduced the level of binding of NF $\kappa$ B-p65 to p38 (Figure 5D, lane 1). In contrast,  $\Delta$ R2 with deletion of amino acids 313–347 did not interfere with association of NF $\kappa$ B-p65 with p38 (Figure 5D, lane 2), indicating that amino acids between positions 279 and 312 are directly responsible for binding. Note that  $\Delta$ R2 successfully immunoprecipitated NF $\kappa$ B-p65 despite what appeared to be a relatively reduced level of expression determined by Western blotting (Figure 5C, lane 2). Also, a faint band for NF $\kappa$ B-p65 in cells treated with the  $\Delta$ R3 mutant (Figure 5D, lane 1) suggests that the deletion in  $\Delta$ R3 may not absolutely abrogate complex formation. Alternatively, the absence of amino acids between positions 279 and 312 may induce a conformational change that prevents binding elsewhere on the p38 molecule.

The MAPK insert is a region formed by two helices in the C-terminal domain that distinguishes MAPKs from members of their superfamily.<sup>36</sup> Others have shown previously that amino acids 294, 295, and 297, deleted in  $\Delta$ R3, are responsible for conformational changes in the p38 MAPK insert upon activation.<sup>36</sup> We generated protein structure models of both mutants using SWISS-MODEL<sup>48</sup> with the crystal structure of p38 $\alpha$  MAP kinase as a template and then visualized the comparisons using UCSF Chimera<sup>50</sup> as shown in Figure 5E. On the basis of our structural analysis and previous reports, the absence of amino acids 294, 295, and 297 in  $\Delta$ R3 may account for the failure to bind NF $\kappa$ B-p65, because without these amino acids, the p38 molecule cannot undergo the required conformational change in the MAPK insert upon activation.

## DISCUSSION

HSP27 has been implicated in diseases ranging from cataract to cancer. HSP27 activation is important to intracellular transport, cytoskeletal architecture, regulation of translation, intracellular redox homeostasis, and protection against spontaneous or stimulated programmed cell death.<sup>56,57</sup> Therefore, HSP27 is an attractive therapeutic target in multiple diseases.<sup>58</sup> Potential tissue specific functions of HSP27 in the cornea have not been elucidated. In intestinal epithelial cells infected with *Entamoeba histolytica*, HSP27 suppresses NF $\kappa$ B activation through interaction with IKK- $\alpha$  and IKK- $\beta$ .<sup>59</sup> However, in other experimental systems, HSP27 enhanced proteasome degradation of I $\kappa$ B to increase the level of nuclear localization of NF $\kappa$ B-p65 and its DNA binding activity.<sup>1</sup> In the studies reported herein, we show that HSP27 is essential for the association of p38 with NF $\kappa$ B-p65 upon viral infection, with important implications for downstream activation of pro-inflammatory mediators.

Using fibroblast-like cells derived from human corneas and infected with a cornea tropic adenovirus, we now demonstrate a critical role for HSP27 in corneal cell signaling and gene expression. In virus-infected cells, knockdown of HSP27 expression was shown to inhibit NF $\kappa$ B-p65 nuclear translocation, possibly by inhibiting I $\kappa$ B function,<sup>1</sup> while nuclear translocation of the p38 MAPK protein was only partially inhibited. These results may indicate an alternative pathway for p38 MAPK in nuclear translocation but could also simply represent shuttling of p38 between the cytoplasm and nucleus through other pathways as previously reported.<sup>3,54</sup> We also demonstrated that knockdown of HSP27 expression reduced the level of chemokine expression similar to chemical inhibition of p38 MAPK,<sup>5</sup> indicating that p38 and HSP27 must have a

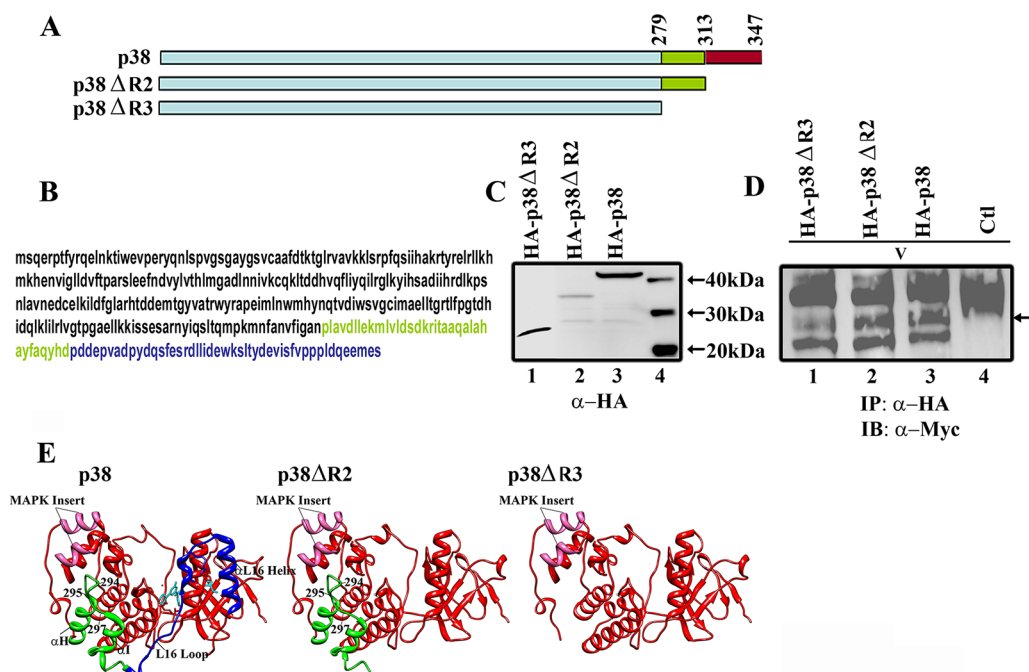


**Figure 5.** Role of p38 amino acids 279–313 in NFκB-p65 binding. (A) Diagram of p38 mutants created by PCR. (B) Amino acid sequence of the p38 molecule. Amino acids deleted in mutants ΔR2 and ΔR3 are colored blue and green, respectively. (C) Western blot showing the cellular expression of transfected ΔR2 and ΔR3. (D) Lysates from cells cotransfected with either HA-tagged p38, HA-p38ΔR2 or HA-p38ΔR3, along with Myc-tagged NFκB-p65, were immunoprecipitated with the anti-HA antibody and immunoblotted with the anti-Myc antibody. As shown, in virus infection Myc-tagged NFκB-p65 coprecipitated (arrow) with both HA-p38 and HA-p38ΔR2, but not HA-p38ΔR3. Lane 4 shows the isotype control. (E) Protein modeling of the p38 ΔR2 and ΔR3 mutants constructed on the basis of homology modeling from the crystal structure of p38 α MAP kinase (PDB entry 1WBS). The N-terminal domain's αL16 helix and L16 loop are deleted in the ΔR2 mutant, colored blue in the intact p38 model. Deletions in the ΔR3 mutant include in addition the C-terminal domain's two helix structures, αH and αI, which are colored green in the intact p38 molecule.

mutual role in chemokine induction. We have not examined whether HSP27 binds directly to the NFκB–p38 complex, but the finding that p38 translocation was not completely inhibited by HSP27 knockdown is suggestive of an indirect mechanism or interaction.

Because both NFκB-p65 and p38 increase their level of nuclear localization upon viral infection, we hypothesized that p38 and NFκB-p65 physically associate to enter the nucleus. Nuclear transport of p38 has been reported previously.<sup>3</sup> Earlier reports also have shown that NFκB activation is inhibited by blocking the p38 pathway.<sup>32</sup> However, ours is the first report to demonstrate a role for HSP27 in nuclear translocation of a p38–NFκB-p65 complex. As there is no nuclear localization signal in the p38 MAPK protein, we considered that p38 nuclear translocation in viral infection might occur because of its association with NFκB-p65. Our experiments using tagged proteins and a NLS mutant of NFκB-p65 showed that NFκB-p65 without its NLS fails to enter the nucleus in viral infection, while the level of translocation of p38 is only partially reduced. Endogenous NFκB-p65 remains a possible mediator of p38 MAPK translocation in this experiment. However, we cannot rule out other mechanisms. Further, we have not yet examined the degree to which these pathways of NFκB activation are specific to viral infection.

Finally, we sought to identify the specific amino acid sequence in p38 responsible for its association with NFκB-p65. For these experiments, we created two C-terminal mutants of p38: ΔR2, a deletion of amino acids 313–347, that lacks the N-terminally oriented domains of the αL16 helix and the L16 loop<sup>47</sup> and ΔR3, a deletion of amino acids 279–347, that also

removes the C-terminal domains of helices αH and αI.<sup>36</sup> Of these two mutants, only ΔR3 prevented NFκB-p65 association upon viral infection. In silico modeling suggested that the deletion of amino acids 294, 295, and 297 in ΔR3 likely prevents the necessary conformational change in the MAPK insert motif region during the activation of p38, where phosphorylation and ATP and other substrate binding normally take place.<sup>36</sup> Experimental confirmation of our in silico modeling would require further examination by crystallography. MAPK insert conformational changes may be necessary for the binding of p38 to NFκB-p65 and subsequent nuclear translocation of NFκB-p65. However, we did not study translocation of NFκB-p65 using the ΔR3 mutant. Also, the amino acid deletions we created in ΔR2 and ΔR3 should increase the level of autophosphorylation of p38, because removal of the L16 loop, deleted in both the ΔR2 and ΔR3 mutants, is known to enhance autophosphorylation.<sup>47</sup> Indeed, Western blot analysis showed increased levels of phosphorylation in ΔR2 and ΔR3 lysates when probed with the antibody against phosphorylated p38 [Y180 (data not shown)].

In summary, we have shown for the first time that amino acids 279–347 of p38 are necessary for its association with NFκB-p65 and for subsequent NFκB-p65 nuclear translocation. These studies suggest that HSP27, p38, and NFκB-p65 function as a signalosome during viral infection.



## AUTHOR INFORMATION

### Corresponding Author

\*The Massachusetts Eye and Ear Infirmary, 243 Charles St., Boston, MA 02114. Telephone: (617) 573-6398. E-mail: james\_chodosh@meei.harvard.edu.

### Funding

This work was supported by National Institutes of Health Grants EY013124, EY021558, and EY014104, a Senior Scientific Investigator Award grant (to J.C.) from Research to Prevent Blindness, Inc. (New York, NY), and the Massachusetts Lions Eye Research Fund.

### Notes

The authors declare no competing financial interest.

## ABBREVIATIONS

HSP, heat shock protein; NF- $\kappa$ B, nuclear factor  $\kappa$ B; MAPKs, mitogen-activated protein kinases; HAdV-D37, human adenovirus type 37.

## REFERENCES

- Parcellier, A., Schmitt, E., Gurbuxani, S., Seigneurin-Berny, D., Pance, A., Chantome, A., Plenchette, S., Khochbin, S., Solary, E., and Garrido, C. (2003) HSP27 is a ubiquitin-binding protein involved in I- $\kappa$ B $\alpha$  proteasomal degradation. *Mol. Cell. Biol.* 23, 5790–5802.
- Rane, M. J., Pan, Y., Singh, S., Powell, D. W., Wu, R., Cummins, T., Chen, Q., McLeish, K. R., and Klein, J. B. (2003) Heat shock protein 27 controls apoptosis by regulating Akt activation. *J. Biol. Chem.* 278, 27828–27835.
- Zheng, C., Lin, Z., Zhao, Z. J., Yang, Y., Niu, H., and Shen, X. (2006) MAPK-activated protein kinase-2 (MK2)-mediated formation and phosphorylation-regulated dissociation of the signal complex consisting of p38, MK2, Akt, and Hsp27. *J. Biol. Chem.* 281, 37215–37226.
- Kappe, G., Franck, E., Verschuure, P., Boelens, W. C., Leunissen, J. A., and de Jong, W. W. (2003) The human genome encodes 10 $\alpha$ -crystallin-related small heat shock proteins: HspB1–10. *Cell Stress Chaperones* 8, 53–61.
- Rajaiya, J., Xiao, J., Rajala, R. V., and Chodosh, J. (2008) Human adenovirus type 19 infection of corneal cells induces p38 MAPK-dependent interleukin-8 expression. *Virology* 37, 17.
- Singh, D., McCann, K. L., and Imani, F. (2007) MAPK and heat shock protein 27 activation are associated with respiratory syncytial virus induction of human bronchial epithelial monolayer disruption. *Am. J. Physiol.* 293, L436–L445.
- Voth, D. E., and Heinzen, R. A. (2009) Sustained activation of Akt and Erk1/2 is required for *Coxiella burnetii* antiapoptotic activity. *Infect. Immun.* 77, 205–213.
- Williams, P. (2007) *Bacillus subtilis*: A shocking message from a probiotic. *Cell Host Microbe* 1, 248–249.
- Okamoto, C. T. (1999) HSP27 and signaling to the actin cytoskeleton focus on “HSP27 expression regulates CCK-induced changes of the actin cytoskeleton in CHO-CCK-A cells”. *Am. J. Physiol.* 277, C1029–C1031.
- Huot, J., Houle, F., Rousseau, S., Deschesnes, R. G., Shah, G. M., and Landry, J. (1998) SAPK2/p38-dependent F-actin reorganization regulates early membrane blebbing during stress-induced apoptosis. *J. Cell Biol.* 143, 1361–1373.
- Piotrowicz, R. S., Hickey, E., and Levin, E. G. (1998) Heat shock protein 27 kDa expression and phosphorylation regulates endothelial cell migration. *FASEB J.* 12, 1481–1490.
- Rousseau, S., Houle, F., Landry, J., and Huot, J. (1997) p38 MAP kinase activation by vascular endothelial growth factor mediates actin reorganization and cell migration in human endothelial cells. *Oncogene* 15, 2169–2177.
- Rocchi, P., Beraldi, E., Ettinger, S., Fazli, L., Vessella, R. L., Nelson, C., and Gleave, M. (2005) Increased Hsp27 after androgen

ablation facilitates androgen-independent progression in prostate cancer via signal transducers and activators of transcription 3-mediated suppression of apoptosis. *Cancer Res.* 65, 11083–11093.

(14) Venkatakrishnan, C. D., Tewari, A. K., Moldovan, L., Cardounel, A. J., Zweier, J. L., Kuppusamy, P., and Ilangoan, G. (2006) Heat shock protects cardiac cells from doxorubicin-induced toxicity by activating p38 MAPK and phosphorylation of small heat shock protein 27. *Am. J. Physiol.* 291, H2680–H2691.

(15) Oya-Ito, T., Liu, B. F., and Nagaraj, R. H. (2006) Effect of methylglyoxal modification and phosphorylation on the chaperone and anti-apoptotic properties of heat shock protein 27. *J. Cell. Biochem.* 99, 279–291.

(16) Son, G. H., Geum, D., Chung, S., Park, E., Lee, K. H., Choi, S., and Kim, K. (2005) A protective role of 27-kDa heat shock protein in glucocorticoid-evoked apoptotic cell death of hippocampal progenitor cells. *Biochem. Biophys. Res. Commun.* 338, 1751–1758.

(17) Sheth, K., De, A., Nolan, B., Friel, J., Duffy, A., Ricciardi, R., Miller-Graziano, C., and Bankey, P. (2001) Heat shock protein 27 inhibits apoptosis in human neutrophils. *J. Surg. Res.* 99, 129–133.

(18) Mehlen, P., Kretz-Remy, C., Preville, X., and Arrigo, A. P. (1996) Human hsp27, *Drosophila* hsp27 and human  $\alpha$ B-crystallin expression-mediated increase in glutathione is essential for the protective activity of these proteins against TNF $\alpha$ -induced cell death. *EMBO J.* 15, 2695–2706.

(19) Freshney, N. W., Rawlinson, L., Guesdon, F., Jones, E., Cowley, S., Hsuan, J., and Saklatvala, J. (1994) Interleukin-1 activates a novel protein kinase cascade that results in the phosphorylation of Hsp27. *Cell* 78, 1039–1049.

(20) Alford, K. A., Glennie, S., Turrell, B. R., Rawlinson, L., Saklatvala, J., and Dean, J. L. (2007) Heat shock protein 27 functions in inflammatory gene expression and transforming growth factor- $\beta$ -activated kinase-1 (TAK1)-mediated signaling. *J. Biol. Chem.* 282, 6232–6241.

(21) Sur, R., Lyte, P. A., and Southall, M. D. (2008) Hsp27 regulates pro-inflammatory mediator release in keratinocytes by modulating NF- $\kappa$ B signaling. *J. Invest. Dermatol.* 128, 1116–1122.

(22) Michaud, S., Marin, R., Westwood, J. T., and Tanguay, R. M. (1997) Cell-specific expression and heat-shock induction of Hsps during spermatogenesis in *Drosophila melanogaster*. *J. Cell Sci.* 110 (Part 17), 1989–1997.

(23) Jantschitsch, C., Kindas-Mugge, I., Metze, D., Amann, G., Micksche, M., and Trautinger, F. (1998) Expression of the small heat shock protein HSP 27 in developing human skin. *Br. J. Dermatol.* 139, 247–253.

(24) Shakoory, A. R., Oberdorf, A. M., Owen, T. A., Weber, L. A., Hickey, E., Stein, J. L., Lian, J. B., and Stein, G. S. (1992) Expression of heat shock genes during differentiation of mammalian osteoblasts and promyelocytic leukemia cells. *J. Cell. Biochem.* 48, 277–287.

(25) Kindas-Mugge, I., and Trautinger, F. (1994) Increased expression of the M<sub>r</sub> 27,000 heat shock protein (hsp27) in vitro differentiated normal human keratinocytes. *Cell Growth Differ.* 5, 777–781.

(26) Spector, N. L., Hardy, L., Ryan, C., Miller, W. H., Jr., Humes, J. L., Nadler, L. M., and Luedke, E. (1995) 28-kDa mammalian heat shock protein, a novel substrate of a growth regulatory protease involved in differentiation of human leukemia cells. *J. Biol. Chem.* 270, 1003–1006.

(27) Pfeffer, L. M. (2011) The role of nuclear factor  $\kappa$ B in the interferon response. *J. Interferon Cytokine Res.* 31, 553–559.

(28) Siggers, R. H., and Hackam, D. J. (2011) The role of innate immune-stimulated epithelial apoptosis during gastrointestinal inflammatory diseases. *Cell. Mol. Life Sci.* 68, 3623–3634.

(29) Gatto, G., Rossi, A., Rossi, D., Kroening, S., Bonatti, S., and Mallardo, M. (2008) Epstein-Barr virus latent membrane protein 1 trans-activates miR-155 transcription through the NF- $\kappa$ B pathway. *Nucleic Acids Res.* 36, 6608–6619.

(30) Huang, J., Ren, T., Guan, H., Jiang, Y., and Cheng, H. (2009) HTLV-1 Tax is a critical lipid raft modulator that hijacks I $\kappa$ B kinases to

the microdomains for persistent activation of NF- $\kappa$ B. *J. Biol. Chem.* 284, 6208–6217.

(31) Pauli, E. K., Schmolke, M., Wolff, T., Viemann, D., Roth, J., Bode, J. G., and Ludwig, S. (2008) Influenza A virus inhibits type I IFN signaling via NF- $\kappa$ B-dependent induction of SOCS-3 expression. *PLoS Pathog.* 4, e1000196.

(32) Rajaiya, J., Sadeghi, N., and Chodosh, J. (2009) Specific NF $\kappa$ B subunit activation and kinetics of cytokine induction in adenoviral keratitis. *Mol. Vision* 15, 2879–2889.

(33) Bardwell, A. J., Frankson, E., and Bardwell, L. (2009) Selectivity of docking sites in MAPK kinases. *J. Biol. Chem.* 284, 13165–13173.

(34) Tanoue, T., Maeda, R., Adachi, M., and Nishida, E. (2001) Identification of a docking groove on ERK and p38 MAP kinases that regulates the specificity of docking interactions. *EMBO J.* 20, 466–479.

(35) Gaestel, M., and Kracht, M. (2009) Peptides as signaling inhibitors for mammalian MAP kinase cascades. *Curr. Pharm. Des.* 15, 2471–2480.

(36) Rodriguez Limardo, R. G., Ferreira, D. N., Roitberg, A. E., Marti, M. A., and Turjanski, A. G. (2011) p38 $\gamma$  activation triggers dynamical changes in allosteric docking sites. *Biochemistry* 50, 1384–1395.

(37) Tanoue, T., Adachi, M., Moriguchi, T., and Nishida, E. (2000) A conserved docking motif in MAP kinases common to substrates, activators and regulators. *Nat. Cell Biol.* 2, 110–116.

(38) Zhou, H., Zheng, M., Chen, J., Xie, C., Kolatkar, A. R., Zarubin, T., Ye, Z., Akella, R., Lin, S., Goldsmith, E. J., and Han, J. (2006) Determinants that control the specific interactions between TAB1 and p38 $\alpha$ . *Mol. Cell. Biol.* 26, 3824–3834.

(39) Jirmanova, L., Sarma, D. N., Jankovic, D., Mittelstadt, P. R., and Ashwell, J. D. (2009) Genetic disruption of p38 $\alpha$  Tyr323 phosphorylation prevents T-cell receptor-mediated p38 $\alpha$  activation and impairs interferon- $\gamma$  production. *Blood* 113, 2229–2237.

(40) Weitzman, M. D., and Linden, R. M. (2011) Adeno-associated virus biology. *Methods Mol. Biol.* 807, 1–23.

(41) Chintakuntlawar, A. V., Astley, R., and Chodosh, J. (2007) Adenovirus type 37 keratitis in the C57BL/6J mouse. *Invest. Ophthalmol. Visual Sci.* 48, 781–788.

(42) Chintakuntlawar, A. V., and Chodosh, J. (2009) Chemokine CXCL1/KC and its receptor CXCR2 are responsible for neutrophil chemotaxis in adenoviral keratitis. *J. Interferon Cytokine Res.* 29, 657–666.

(43) Chintakuntlawar, A. V., Zhou, X., Rajaiya, J., and Chodosh, J. (2010) Viral capsid is a pathogen-associated molecular pattern in adenovirus keratitis. *PLoS Pathog.* 6, e1000841.

(44) Robinson, C. M., Shariati, F., Gillasp, A. F., Dyer, D. W., and Chodosh, J. (2008) Genomic and bioinformatics analysis of human adenovirus type 37: New insights into corneal tropism. *BMC Genomics* 9, 213.

(45) Natarajan, K., Rajala, M. S., and Chodosh, J. (2003) Corneal IL-8 expression following adenovirus infection is mediated by c-Src activation in human corneal fibroblasts. *J. Immunol.* 170, 6234–6243.

(46) Chodosh, J., Astley, R. A., Butler, M. G., and Kennedy, R. C. (2000) Adenovirus keratitis: A role for interleukin-8. *Invest. Ophthalmol. Visual Sci.* 41, 783–789.

(47) Diskin, R., Lebendiker, M., Engelberg, D., and Livnah, O. (2007) Structures of p38 $\alpha$  active mutants reveal conformational changes in L16 loop that induce autophosphorylation and activation. *J. Mol. Biol.* 365, 66–76.

(48) Arnold, K., Bordoli, L., Kopp, J., and Schwede, T. (2006) The SWISS-MODEL workspace: A web-based environment for protein structure homology modelling. *Bioinformatics* 22, 195–201.

(49) Burmeister, W. P., Guilligay, D., Cusack, S., Wadell, G., and Arnberg, N. (2004) Crystal structure of species D adenovirus fiber knobs and their sialic acid binding sites. *J. Virol.* 78, 7727–7736.

(50) Pettersen, E. F., Goddard, T. D., Huang, C. C., Couch, G. S., Greenblatt, D. M., Meng, E. C., and Ferrin, T. E. (2004) UCSF Chimera: A visualization system for exploratory research and analysis. *J. Comput. Chem.* 25, 1605–1612.

(51) Bonizzi, G., and Karin, M. (2004) The two NF- $\kappa$ B activation pathways and their role in innate and adaptive immunity. *Trends Immunol.* 25, 280–288.

(52) Dev, A., Iyer, S., Razani, B., and Cheng, G. (2011) NF- $\kappa$ B and innate immunity. *Curr. Top. Microbiol. Immunol.* 349, 115–143.

(53) Carlotti, F., Dower, S. K., and Qvarnstrom, E. E. (2000) Dynamic shuttling of nuclear factor  $\kappa$ B between the nucleus and cytoplasm as a consequence of inhibitor dissociation. *J. Biol. Chem.* 275, 41028–41034.

(54) Wu, R., Kausar, H., Johnson, P., Montoya-Durango, D. E., Merchant, M., and Rane, M. J. (2007) Hsp27 regulates Akt activation and polymorphonuclear leukocyte apoptosis by scaffolding MK2 to Akt signal complex. *J. Biol. Chem.* 282, 21598–21608.

(55) Wang, Z., Harkins, P. C., Ulevitch, R. J., Han, J., Cobb, M. H., and Goldsmith, E. J. (1997) The structure of mitogen-activated protein kinase p38 at 2.1-Å resolution. *Proc. Natl. Acad. Sci. U.S.A.* 94, 2327–2332.

(56) Kostenko, S., and Moens, U. (2009) Heat shock protein 27 phosphorylation: Kinases, phosphatases, functions and pathology. *Cell. Mol. Life Sci.* 66, 3289–3307.

(57) Holzbaur, E. L., and Scherer, S. S. (2011) Microtubules, axonal transport, and neuropathy. *N. Engl. J. Med.* 365, 2330–2332.

(58) Kessler, T., Hamprecht, K., Feuchtinger, T., and Jahn, G. (2010) Dendritic cells are susceptible to infection with wild-type adenovirus, inducing a differentiation arrest in precursor cells and inducing a strong T-cell stimulation. *J. Gen. Virol.* 91, 1150–1154.

(59) Kammanadiminti, S. J., and Chadee, K. (2006) Suppression of NF- $\kappa$ B activation by *Entamoeba histolytica* in intestinal epithelial cells is mediated by heat shock protein 27. *J. Biol. Chem.* 281, 26112–26120.